EFFECT OF SPINEL ADDITION ON THE SINTERING BEHAVIOR AND MICROSTRUCTURE OF ALUMINA-SPINEL CERAMICS

EMRE YALAMAÇ

Celal Bayar University, Department of Materials Engineering, 45140 Manisa, Turkey

E-mail: emre.yalamac@cbu.edu.tr

Submitted June 13, 2014; accepted November 20, 2014

Keywords: Alumina, Magnesium Aluminate Spinel, Ceramic Composite, Densification, Hardness

Sintering behaviors of alumina-spinel powder mixtures were investigated up to 1600°C using a vertical dilatometer. Final density and microstructure of pure alumina, magnesium aluminate spinel ($MgAl_2O_4$) ceramics and ceramic composites with different alumina-spinel ratio were examined. As a result, the densification and final density of alumina-spinel composites were affected by addition of 10 wt. % and 20 wt. % spinel into alumina. Non-stoichiometric alumina-rich spinel phase was detected in the matrix of the composites by EDS. The presence of spinel phase inhibited alumina grain growth, therefore the pure alumina sample had nearly twice the grain size as the multiphase alumina-spinel samples. Vickers hardness of the samples was tested and compared. The hardness of the composite with 10 wt. % spinel was slightly higher than the pure alumina ceramic, due to grain size and density of the samples.

INTRODUCTION

Magnesium aluminate spinel ($MgAl_2O_4$) possesses a high-melting point, high chemical inertness against both acidic and basic slags, and low expansion values at elevated temperatures. It is also well known for quite a long time that alumina–magnesia spinel composites with varying amounts of alumina and magnesia (either alumina-rich or magnesia-rich) are very important refractory composite materials for various interesting applications in the metallurgical and cement industries. Generally, MgO-spinel bricks are preferred for cement rotary kilns whereas Al_2O_3-spinel castables are preferred for steel ladles. This is due to the fact that the dense alumina-magnesia spinel has adequate 'hot strength', high 'corrosion resistance' to both acidic and basic slags, and also good erosion resistance at elevated temperatures [1-3].

Investigation of Al_2O_3 and $MgO{\cdot}Al_2O_3$ composites should start with the phase equilibrium diagram [4]. The binary phase diagram $MgO/MgAl_2O_4/Al_2O_3$ is a very important yet relatively simple system in ceramics (Figure 1). There is negligible solubility for Mg^{2+} in corundum while there is significant room for solid solubility of both Mg^{2+} and Al^{3+} in spinel. For example, when alumina is mixed with spinel and heated up to 1600°C, Al^{3+} is expected to diffuse into spinel until an alumina rich spinel with 81 wt. % Al_2O_3 is formed. However, alumina–magnesia spinel composites with varying ratio of alumina and spinel are formed in the alumina-spinel multiphase region.

Pal et al., in a relevant study [5] investigated the sintering behaviour of alumina-spinel composites. They prepared different batch compositions containing spinel and calcined alumina and then green compacts were produced by uniaxial pressing. The pellets were classically sintered between 1500 and 1600°C for 2 hours. Apparent porosity and bulk density of sintered pellets were measured by the Archimedes method. Firing shrinkage and densification percentage were calculated from dimensions of the green and sintered pellets. They observed that an addition of 5 - 10 wt. % alumina in spinel causes a considerable increase in sintered bulk

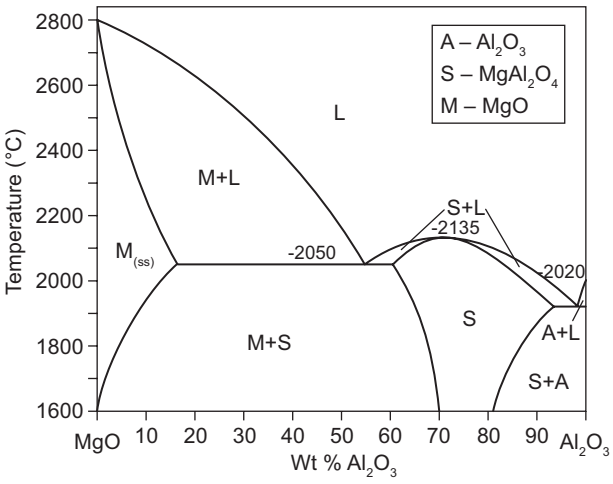

Figure 1. The $MgO–Al_2O_3$ phase diagram [4].

density. On the other hand, further addition of alumina causes a gradual decrease in the bulk density, which is unexpected, since the true specific gravity of alumina is greater than that of spinel. They explained that the sintered density of pellets made only of calcined alumina gives a lower value, which reveals that calcined alumina is not so reactive. Microstructural inhomogeneity was observed in SEM images of most of the composites made by the interaction of spinel and calcined alumina at 1600°C.

In this study the sintering behaviour and microstructure formation of multiphase alumina-spinel ceramic composites were investigated. The high temperature interaction between spinel and alumina was represented by the change in final microstructural and mechanical properties such as hardness of the ceramic composites.

EXPERIMENTAL

In this study, commercially available magnesium aluminate spinel ($MgAl_2O_4$) powder and submicron α-alumina powder were used for production of alumina spinel ceramic composites. Both the alumina powder (BMA15) and the spinel powder (S30-CR) were Baikowski products. Some physical and chemical properties of the powders are shown in Table 1.

In order to investigate the effects of spinel phase on the microstructural and mechanical properties of alumina spinel ceramics, spinel powder and alumina powder were mixed with different weight ratio. The powders were mixed in an agate mortar with addition of some ethanol and PVA binder for 30 minutes.

Table 1. Some physical and chemical properties of powders [6].

		Alumina (BMA15)	Spinel (S30-CR)
d_{50} (μm) by Sedigraph$^+$ or laser diffraction*		0.15*	0.2$^+$
Specific surface area BET ($m^2 \cdot g^{-1}$)		16	31
d_{BET} (μm) calculated from BET data		0.113	0.055
Chemical analysis (ppm)	Na	12	10
	Fe	6	10
	Si	10	20
	Ca	2	5
	K	20	–

Table 2. Designation of powder mixtures.

Sample code	Materials combination
C100	100 wt. % alumina
C90	90 wt. % alumina + spinel
C80	80 wt. % alumina + spinel
C0	100 wt. % spinel

To produce green cylindrical (10 mm diameter) compacts, powder or powder mixtures were pressed at 250 MPa with single-action mode of uniaxial pressing. The green compacts produced and their mixing ratio are shown in Table 2. In order to examine the sintering behavior of the powder and powder mixtures, they were sintered in a high temperature vertical dilatometer (L75V, Linseis) at 1600°C for 1 hour soaking with 10°C·min^{-1} of heating rate under static air atmosphere. The sintered samples were cooled in the dilatometer with a cooling rate of 20°C min^{-1}.

Final bulk densities of the sintered pellets were measured and calculated using the Archimedes principle as described in ASTM standard C373-88. In this technique, the final density of ceramic was determined by measuring the weight of a specimen in air (dry mass), in distilled water (suspended mass) and the water-saturated sample again in air (saturated mass) at room temperature.

In order to measure the final density of sintered alumina-spinel ceramics, theoretical densities of powder mixtures were calculated according to mixture ratio. They were calculated basically with the following equation,

$$\rho_{mixture} = \rho_{th(spinel)} \text{ vol. \% spinel} + \\ + \rho_{th(alumina)} \text{ vol. \% alumina} \quad (1)$$

Theoretical densities of spinel and alumina were taken as 3.55 and 3.987 g·cm^{-3}, respectively [7].

Densification [$\rho(T)$] and densification rate ($d\rho/dT$) curves were calculated and plotted from the recorded shrinkage data and the final density of samples (ρ_f) by using the following equations:

$$\rho(T) = \rho_f \left(\frac{1 + \frac{\Delta L_f}{L_o}}{1 + \frac{\Delta L(T)}{L_o}} \right)^3 \quad (2)$$

in which L_o is the initial sample length, L_f is the final sample length and $L(T)$ is the sample length at the temperature (T) [8]. To obtain the densification rate, temperature derivative of relative density ρ is taken,

$$\frac{d\rho(T)}{dT} = -3 \times \frac{d\left(\Delta L(T)/L_0\right)}{dT} \times \frac{\left(1 + \frac{\Delta L_f}{L_0}\right)^3}{\left(1 + \frac{\Delta L(T)}{L_0}\right)^4} \times \rho_f \quad (3)$$

The crystalline phases were identified by X-ray diffraction analysis (D2 Phaser, Bruker).

In order to investigate the microstructures of the sintered pellets, they were cut parallel to the cylindrical axis into two parts. Half of them were mounted into polyester resin before being ground and polished by conventional sample preparation methods. To reveal the morphology and microstructural alteration in the

samples, the other half of samples were ground and polished by hand before thermally etched at about 100°C below the sintering temperature. Microstructures of the polished and thermally etched surfaces were observed by SEM (scanning electron microscope, Quanta 250, FEI). The average grain size was determined from SEM micrographs by a surface intercept method ($d = 1.38\sqrt{s}$, where s is the intercepted surface of grains) [9]. Since the grain size couldn't be precisely evaluated from fracture surface micrographs, the measurements were done from etched surfaces.

Chemical compositions of the present phases were examined by energy-dispersive X-ray spectroscopy (EDS) (x-act EDAX, Oxford Instruments).

Vickers indentation hardness of ceramics were measured from metallographically prepared surfaces of the samples, with universal macro hardness test equipment (Duravision 20, EMCOTEST) using a loading of 9.81 N for 15 seconds (ASTM C 1327–03). Due to the possible presence of multiphase ceramics that are not homogeneous, nor not fully dense, ten acceptable indentations were made.

RESULTS AND DISCUSSION

The final densities of the samples are given in Table 3. Relative densities of the samples were calculated by division of the Archimedes bulk density by the theoretical density.

Table 3. Archimedes bulk densities.

	Bulk density	Theoretical density (calculated)	Relative density (%)
C100	3.926	3.987	98.458
C90	3.892	3.939	98.816
C80	3.829	3.891	98.393
C0	3.402	3.550	95.831

Densification and densification rate curves of the samples during sintering with 10°C·min^{-1} heating rate up to 1600°C are given in Figure 2. The upper curves show the densification of the samples. Except for the pure spinel sample (C0), all samples show the same densification behavior and nearly the same final density. According to the results, the densification rate curves start at around 1000°C for all samples and the maximum densification rate of the samples corresponding to the maximum peak, changes with sample composition. The maximum densification rate of the C100 sample is around 1315°C and it has the lowest peak temperature. When the spinel content increases, the maximum densification rate temperature also increases from 1315 to 1365°C. On the other hand, a pure spinel shows extremely different densification behaviour than the other samples. It has a very broad plateau type peak between 1300°C and 1420°C, a behaviour that is obviously characteristic of this commercial spinel powder. Since the powder was in an agglomerated form and the primary particle size was in the nano range, the particle size distribution is not monomodal [10]. This sample also has the lowest final density. The melting temperature of spinel (2135°C) is higher than that of alumina (2053°C), therefore densification rate of spinel is lower than alumina [7]. Nevertheless, in contrast to what is expected, here the addition of spinel into alumina does not decrease the densification and the final density of alumina-spinel composites (in Table 3).

Figure 3 shows XRD patterns of sintered samples, after sintering of pure alumina and spinel powders, only spinel and alumina phases were detected on the XRD patterns of C0 and C100, respectively. But addition of spinel powder into alumina powder strongly affected the XRD patterns of sintered samples. Spinel was detected as a second phase and, as expected, when the content of spinel powder is increased, intensity of spinel phase increases in the patterns.

Figure 4 shows SEM images of polished and thermally etched surfaces pure spinel (Figure 4a) and

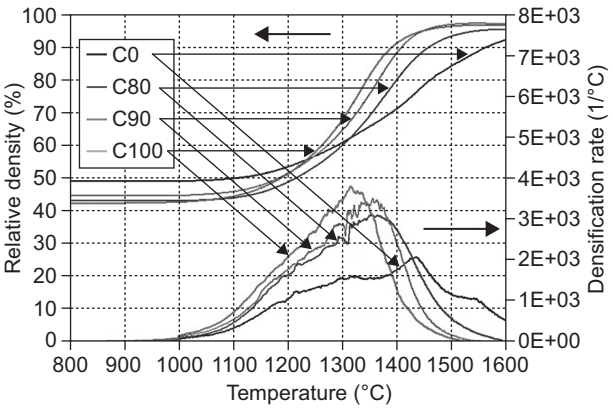

Figure 2. Densification and densification rate curves of samples during sintering with 10°C·min^{-1} heating rate up to 1600°C for 1 hour; the upper curves are relative densities, and the lower curves are their temperature derivatives, $d\rho/dT$.

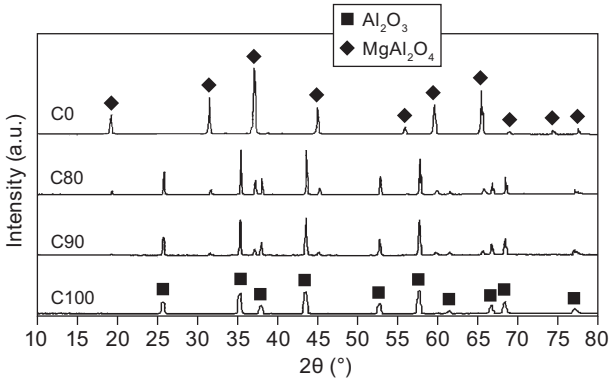

Figure 3. XRD patterns of the sintered samples.

alumina (Figure 4b) microstructures, respectively. The initial spinel powders have a very fine particle size, as mentioned in the experimental part, therefore in the final microstructures, spinel has only 0.8 μm average grain size, while pure alumina has larger grain size and its average grain size is around 6.2 μm. Figures 4 c and d show the microstructures for the C80 and C90 samples, respectively. According to these images, the alumina grain size of the samples was roughly measured and a grain size of 3.3 μm was found, nearly the same in both cases. Thus, pure alumina phase sample has nearly twice the grain size as the multiphase of alumina-spinel composites. This means that spinel phase inhibited alumina grain growth. This result is in agreement with a previous study of the author [11].

In order to detect elements of present phases in the multiphase alumina-spinel samples, EDS analyses were done. Figure 5 displays the EDS analyses of C80 samples from different regions of spinel (S) and alumina (A). According to the EDS analysis of A region, alumina is the present phase in this region and, magnesia aluminate spinel phase is the present phase in the S region. Spinel phase stoichiometrically contains 16.9 wt. % Mg and 38.0 wt. % Al, but the EDS analysis showed that there are 11.5 wt. % Mg and 42.5 wt. % Al present in the S region. Similar EDS results were measured in the C90 sample, with the Al ratio slightly higher than in the C80 sample as expected. Excess alumina in non-stoichiometric spinel can be accommodated in different ways, e.g. via introduction of a substitution defect on the tetrahedral magnesium sites and an aluminum vacancy or magnesium vacancy to compensate for the excess positive charge [12,13].

To compare hardness of the samples, ten indentation

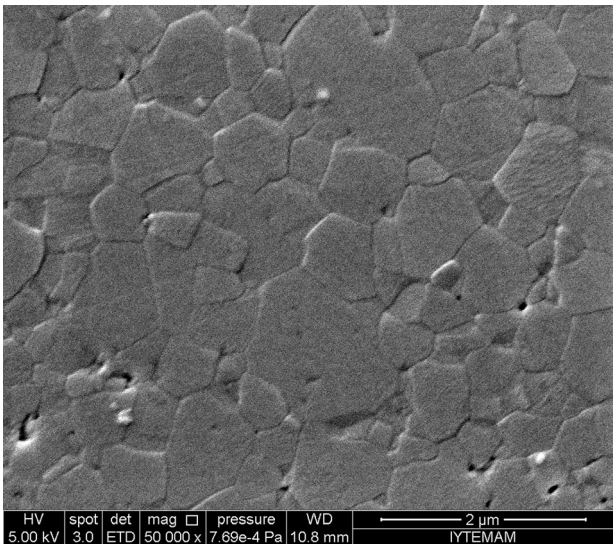

a) C0

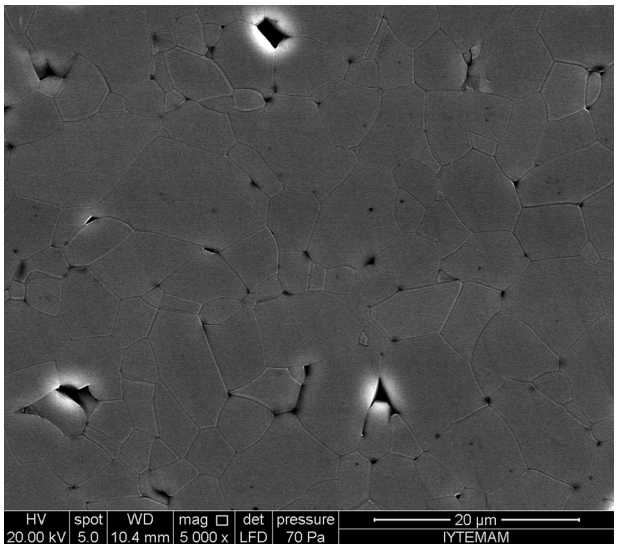

b) C100

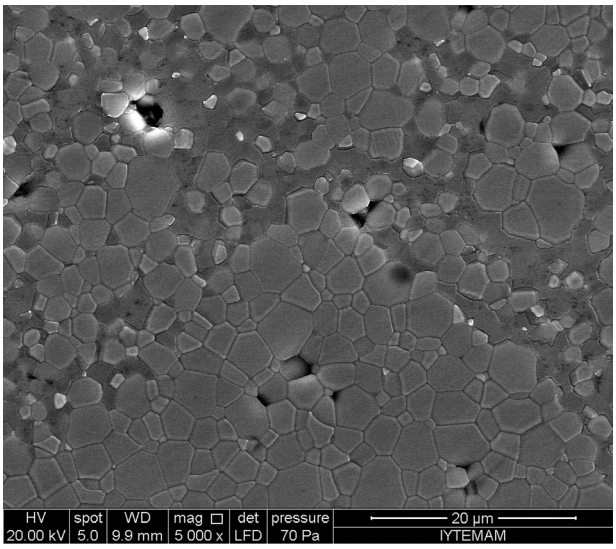

c) C80

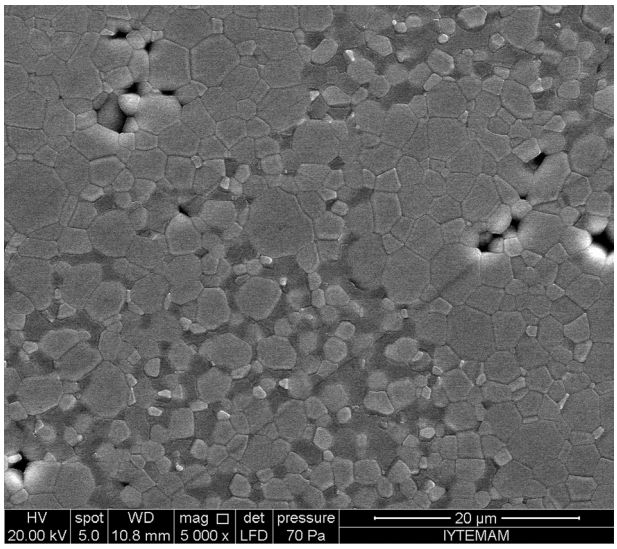

d) C90

Figure 4. SEM micrographs of the samples a) C0, b) C100, c) C80, and d) C90.

results are given in Figure 6 with standard deviations. In order to statistically describe the uncertainty in the hardness measurements, the standard deviations were calculated from ten acceptable indentations. According to results C90 sample has the highest hardness value and C0 has the lowest one. Comparing the hardness of alumina-spinel ceramic composites, hardness of C90 sample is seen higher than C100 and C80. Although, C90 and C80 samples have nearly same alumina grain size, C90 has slightly higher bulk density than C80. Therefore C90 has higher hardness value than C80 sample. In literature, hardness commonly decreases with decreasing grain size for larger grain sizes, Tani et al, [14] showed that a marked decrease in hardness with decreasing grain size from 60 to 6 μm for Al_2O_3 at low Hv (2 N load) but for fine grain sizes, hardness generally increases with decreasing grain sizes e.g. due to Hall-Petch type effects on the associated plastic flow [15]. Addition of spinel into alumina decreases the grain size of alumina from ~ 6 to ~ 3 μm. This means that small amounts of spinel addition to alumina increase the hardness of alumina ceramics. Therefore, alumina spinel ceramic composites can have higher mechanical properties than pure alumina ceramics.

Figure 7 shows Vickers indentation regions of C80 sample in the matrix region (Figure 7a) and in alumina region (Figure 7b). The continuous matrix region was found to be composed of spinel and alumina grains while the discontinuous phase of rounded shapes was composed of only alumina grains, these rounded shapes were 60 – 80 μm in size. The hardness of the matrix region is 17.3 GPa, but the hardness of the alumina region is 18.3 GPa. According to Figure 6, hardness of C80 is about 17.6 GPa. The hardness of pure spinel region is about 12.6 GPa (Figure 6), see also [16] therefore the matrix of the composites consists of non-stoichiometric alumina rich-spinel and alumina phases.

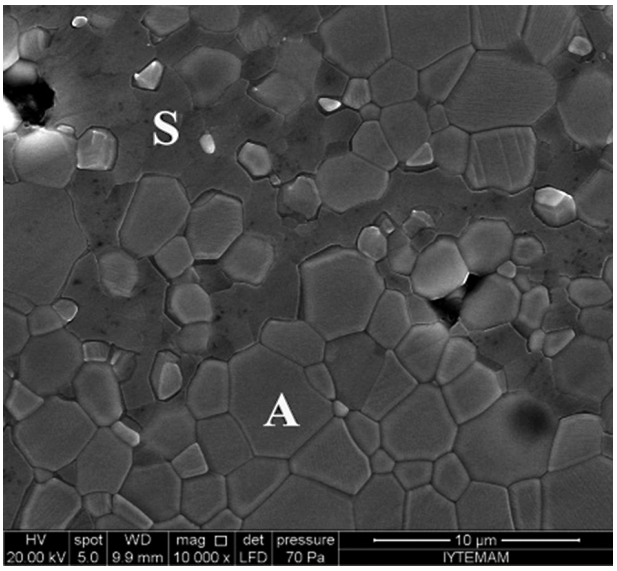

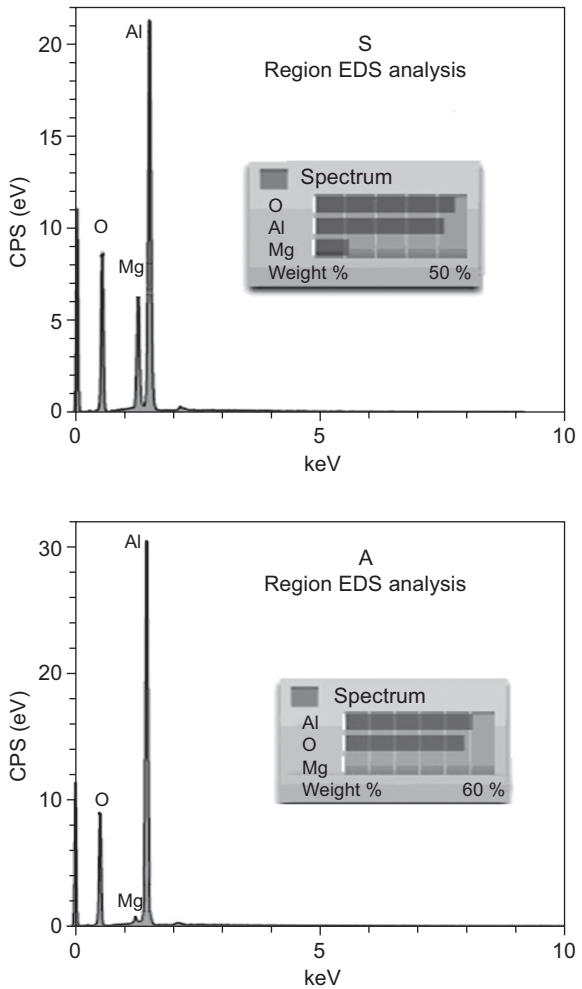

Figure 5. EDS analyses of C80 sample at different regions (S: Spinel and A: Alumina regions).

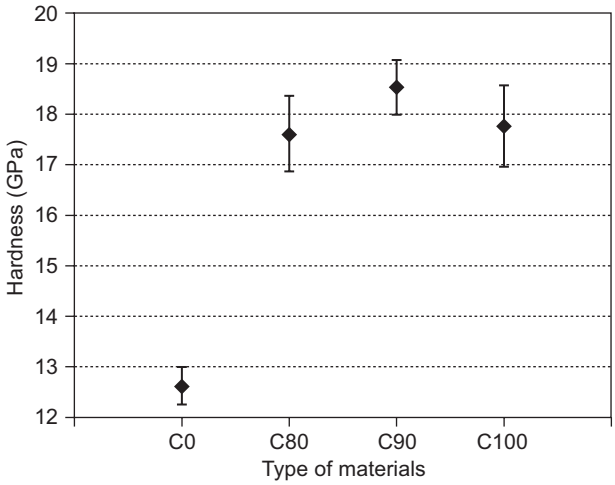

Figure 6. Hardness of the samples (error bars are standard deviation limits).

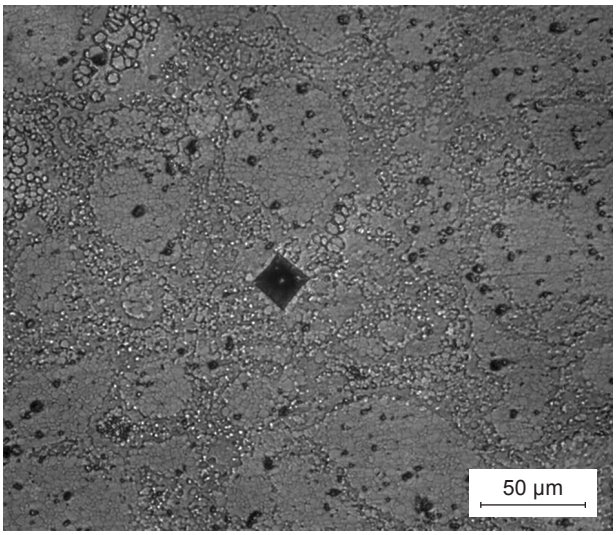

a) matrix

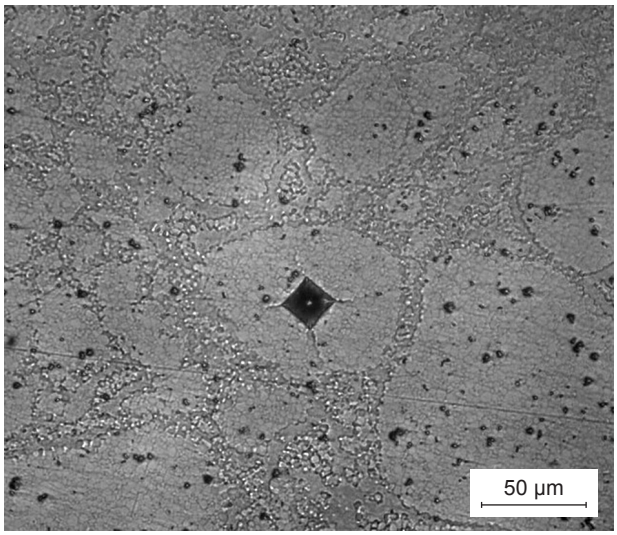

b) alumina parts

Figure 7. Vickers Indentation of a) matrix and b) alumina parts of C80 sample.

CONCLUSIONS

When alumina and spinel are mixed and sintered together, a compact ceramic with high density could be produced. All samples except for the pure spinel showed similar densification behavior and almost the same final density. Pure spinel lagged a little behind in densification upon heating due to its higher melting point. XRD analysis indicated that both phases retain their crystallinity.

Spinel addition strongly affects the microstructure, especially the final grain size of the alumina phase. As expected, addition of spinel into alumina decreases grain size. The Vickers hardness of composites with 10 wt. % spinel is slightly higher than that of the pure alumina ceramic, evidently due to the restricted grain growth in the composite.

REFERENCES

1. Mori, J., Watenabe, W., Yoshimura, M., Oguchi, Y., Kawakami, T.: Bull. Am. Ceram. Soc. *69*, 1172 (1990).
2. Ganesh, I., Bhattacharjee *S.*, Saha B.P., Johnson R., Rajeshwari K., Sengupta R., Ramana Rao M.V., Mahajan Y.R.: Ceram. Int. *28*, 245 (2002).
3. Ko, Y.: Ceram. Int. *28*, 805 (2002).
4. Carter, C., Norton, M.: *Ceramic Materials Science and Engineering*, 2nd ed., p.127, Springer, New York 2007.
5. Pal, S., Bandyopadhyay, A. K., Pal, P. G., Mukherjee, S. & Samaddar, B. N.: Bull. Mater. Sci. *32*, 169 (2009).
6. Baikowski. Available from: http://www.baikowski.com [accessed 10.01.14].
7. Rahaman, M.: *Ceramic Processing and Sintering*, 2nd ed., p.855-857, Marcel Dekker Inc., New York 2003.
8. Legros, C., Carry, C., Bowen, P., Hofmann, H.: J. Eur. Ceram. Soc. *19*, 1967 (1999).
9. Charmond S., Carry C.P., Bouvard D.: J. Eur. Ceram. Soc. *30*, 1211 (2010).
10. Yalamaç, E.: PhD Thesis, Izmir Institute of Technology-Grenoble University, (2010).
11. Yalamac, E., Carry, C., Akkurt, S.: J. Eur. Ceram. Soc. *31*, 1649 (2011).
12. Okuyama Y., Kurita N, F. N.: Solid State Ionics *177*, 59 (2006).
13. Ting C.J., Lu H.Y.: J Am Ceram Soc. *82*, 841 (1999).
14. Tani T., Miyamoto Y., Koizumi M., Shimada M.: Ceram. Int. *12*, 33 (1986).
15. Rice R.W., Wu C.C., Borchelt F.: J. Am. Ceram. Soc. *77*, 2539 (1994).
16. Maca, K., Trunec, M., Chmelik, R.: Ceram. Silikaty *51*, 94 (2007).